



13TH CANADIAN MASONRY SYMPOSIUM
HALIFAX, CANADA
JUNE 4TH – JUNE 7TH 2017



TALL MASONRY WALLS WITH IN-LINE BOUNDARY ELEMENTS

Entz, Joseph¹; Cruz Noguez, Carlos²; Guzmán Sánchez, Odín³ and Banting, Bennett⁴

ABSTRACT

Tall, slender masonry walls are a competitive solution in both low and high-rise structures to resist out-of-plane and gravity loads. The use of taller and thinner walls is appealing due to the use of less material, need for smaller foundations, faster construction, lower seismic forces, and the ability to create more interior space. However, the design of conventional tall walls for out-of-plane bending according to CSA S304-14 for masonry structures tends to have practical limits related to their axial load capacity, buckling stability, and reinforcement details. Most conventional masonry walls rely on a single reinforcement bar placed at the centre of the unit, and designers that opt for multiple layers of reinforcement or non-conventional units seeking to enhance wall strength and stiffness are hindered by empirical limits in the S304 standard. A new type of masonry slender wall based on a similar concept of seismic boundary elements is proposed in this study. These ‘in-line boundary elements’ act as localized regions of strength and stiffness by providing tied reinforcement in two layers close to the surface of the wall. Results of ongoing experimental tests on masonry prisms containing pre-tied steel reinforcement cages and specially designed masonry units to fit around the cages are presented. The results show that the cage has a beneficial effect on the structural integrity of the confined core of reinforced prisms. Plane-section compatibility analysis is used to compare the performance of the reinforcing cage compared to conventional design scenarios with varying amounts of reinforcement placed at the middle of the section. A preliminary finite-element analysis model developed for tall masonry walls is also presented.

KEYWORDS: *slender wall, out-of-plane, boundary element, prism testing*

INTRODUCTION

The provisions for out-of-plane (OOP) loadbearing slender walls in the masonry code of Canada [1] ensure that walls will have a ductile behaviour, with significant deformation before the crushing

¹ MSc student, University of Alberta, 116th St. & 85th Ave., Edmonton, AB, Canada, jentz@ualberta.ca

² Assistant Professor, University of Alberta, 116th St. & 85th Ave., Edmonton, AB, Canada, cruznogu@ualberta.ca

³ PhD student, University of Alberta, 116th St. & 85th Ave., Edmonton, AB, Canada, guzmansa@ualberta.ca

⁴ Masonry Research and Development Engineer, Canada Masonry Design Centre, 360 Superior Blvd., Mississauga, ON, Canada, bbanting@canadamasonrycentre.com

of the masonry and no buckling failures. Meeting these code provisions for some applications requires the use of thicker and/or stronger blocks to increase the bearing area and stiffness, adding compressive steel reinforcement, or increasing the effective depth of the provided tension reinforcement [1]. This often translates into a thicker, more expensive, and impractical wall to construct given architectural and engineering demands for space, size, and loads.

To improve the performance of OOP, reinforced masonry (RM) walls, several techniques have been used. Full-scale tests indicate that staggered, vertical reinforcing bars produce a higher energy absorption capacity and displacement ductility in comparison to conventional reinforcing bars placed at the mid-depth [2]. Near-Surface Mounted (NSM) tension reinforcement methods consisting of placing reinforcement bars (made of stainless steel or FRP) on the tensile side of walls can effectively improve the OOP strength, and rigidity of unreinforced masonry walls [3]. In unreinforced masonry (URM) walls, the addition of Fibre Reinforced Polymer (FRP) rebar in quantities as low as 0.006% has resulted in a 25% increase in lateral load capacity and a 200-400% increase in lateral energy absorption [4]. Steel bars strategically positioned in grooves on the exterior surface of CMU walls are more effective than other NSM reinforcing techniques such as FRP strip sheets [5]. These methods, however, present challenges in the context of fire-resistance and cost, and do not improve the buckling strength of the wall.

Confined boundary elements are an effective method for improving the in-plane seismic response of in-plane walls, by enhancing the structural integrity of the regions of the wall under compression. Tied rebar “cages” are provided at the ends of the walls with the purpose of confining the grout and masonry materials inside the ties, preventing buckling of the longitudinal reinforcement, and enhancing the ductility of the system by facilitating yielding of the tension steel. Studies of masonry shear walls with reinforced boundary elements have shown that the in-plane performance under seismic loading is significantly better in comparison to control walls with no boundary elements [6]. Other observations include a delay in rebar buckling and grout crushing. Integral, concrete, in-line boundary elements in masonry walls have been documented to increase in-plane ductility by up to 48% and the total energy dissipation capacity by up to 260% in comparison to similar masonry walls without in-line boundary elements [7]. The 2014 edition of CSA S304 allows for the design of masonry shear walls with in-line boundary elements as a Seismic Force Resisting System (SFRS) [8].

This paper presents a pilot study on the use of in-line boundary elements in OOP masonry walls. The system consists of a pre-tied reinforcement cage that fits in one masonry unit, effectively becoming a “concealed column”. The system is used in combination with specially designed units able to slide around the cage. The in-line boundary elements act as regions of localized strength and stiffness, increasing the buckling strength and reducing second order effects. Under significant axial loads, the reinforcement in compression in the cage will likely increase ductility in OOP walls. This paper focuses on concentric tests conducted on 5-unit prisms reinforced with a reinforcing cage. The results are discussed in terms of feasibility of construction, strength, structural performance, and failure modes.

EXPERIMENTAL SETUP

To explore the performance of the in-line boundary elements, prism behaviour was investigated first. Two batches of 15 masonry prisms each were built at the University of Alberta. All prisms were 5 courses high, made with 20cm, 15 MPa (nominal strength) lintel and half lintel blocks and S-type mortar. The dimensions of the constructed prisms are 190mm x 390mm x 990mm (Fig. 1). From these, 15 were tested under concentric loads and 15 will be tested under eccentric loads. The prisms were tested on an MTS hydraulic press with a maximum axial capacity of 6,200 kN. Experienced masons conducted the fabrication of the prisms. The construction process used in the fabrication of these prisms containing a reinforcing cage showed no significant variations from conventional masonry practices followed in the construction of walls.

The pre-tied reinforcing cages were fabricated with 4-10M (11.3 mm diam.) bars as longitudinal reinforcement and 6.34 mm smooth wire ties spaced at 150mm c/c. The spacing of the ties was chosen to prevent buckling of the longitudinal reinforcement. According to S304-14, tie spacing should be the lesser of 16 times the diameter of the longitudinal bar (181mm), 48 times the diameter of the tie (304 mm), or the least dimension of the member (190 mm).

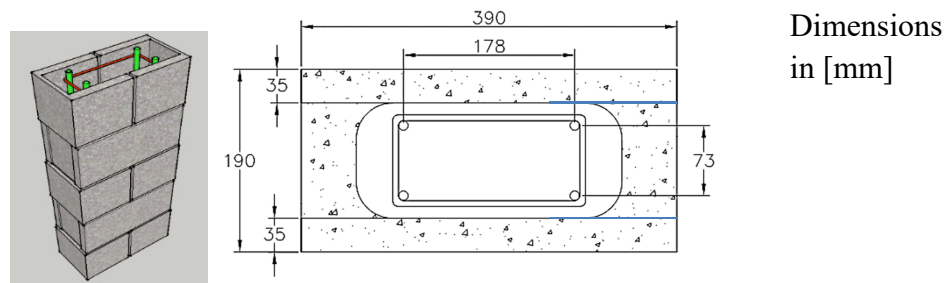


Figure 1: Typical Prism Construction

Ancillary tests conducted on grout and mortar samples indicate a 28-day mortar strength of 12.5 MPa and 28-day grout strength of 30 MPa. The yield strength of the rebar was determined to be 420 MPa.

Concentric Testing

To investigate the response of the prisms under pure axial load, obtain the masonry strength, and to evaluate the behaviour of the cage separately, three prism types were tested concentrically: 4 hollow, 5 grouted (unreinforced), and 4 grouted (reinforced). Prior to testing, the prisms were capped with plaster. Two prisms were not tested due to failures during construction and transportation.

Eccentric Testing

Fifteen reinforced prisms were constructed for eccentric testing to investigate the response of the prisms with reinforcing cages under a combination of axial loads and OOP bending moments. Three eccentricities were selected for investigation: $t/6$, $t/3$, and $5t/12$, as suggested by previous research [9]. Unfortunately, after removing the formwork it was found that most prisms from this

batch had large voids caused by insufficient grout penetration, with the rebar being exposed in some cases. An attempt was made to repair the prisms with a low-viscosity, fast-setting mortar prior to testing. However, the resulting non-homogeneity made it infeasible to assess the performance of these repaired prisms. In the following section, only the performance of six prisms with no fabrication defects will be discussed. The response of repaired specimens will be discussed only qualitatively. The eccentric load setup consists of two steel bearing plates, attached to square steel bars to produce the desired eccentricity (Fig. 2). At both top and bottom, knife edge assemblies provide a pin support condition.

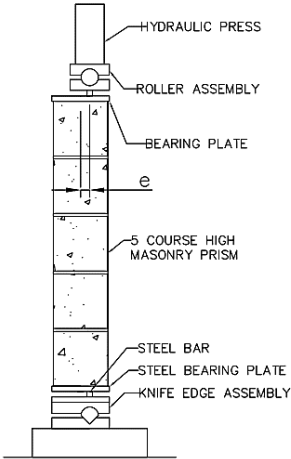


Figure 2: Eccentric Testing Setup

CONCENTRIC TEST RESULTS

The representative failure mode for the three different prism types is shown in Fig. 3. Failure of the hollow prisms was initiated by a vertical crack in the web followed by a face shell cracking with increased loading. Failure of the grouted, unreinforced prisms was characterised by significant cracking on all 4 sides in various directions. The face shells and core both cracked, with the prisms separating into two or more pieces at the ultimate load. In the reinforced prisms, the confined core remained intact while the surrounding unconfined masonry spalled. Face shell cracking was observed in reinforced prisms prior to ultimate load and complete separation of face shell masonry was observed at ultimate load.

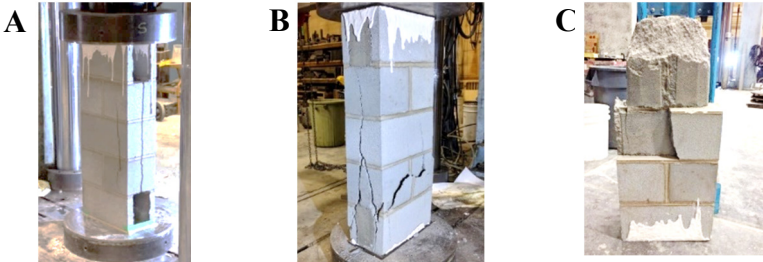


Figure 3: Prism Failure Mode – Hollow (A), Grouted Unreinforced (B), Grouted Reinforced (C)

Rebar buckling was observed in two of the reinforced prisms. Strain measurements showed that the rebar buckled before reaching the yield strain (at peak load), when significant damage in the grouted core had occurred and the face shells had cracked (Fig. 4). As noted earlier, the ties were spaced at 150 mm which is a spacing less than that required in S304-14 (181 mm). Since one of the design objectives in this project is to enhance the strength and stiffness of a wall element through the use of a rebar cage and a confined grout core in the boundary element, future phases of this project will investigate the performance of prisms with varying tie spacing.

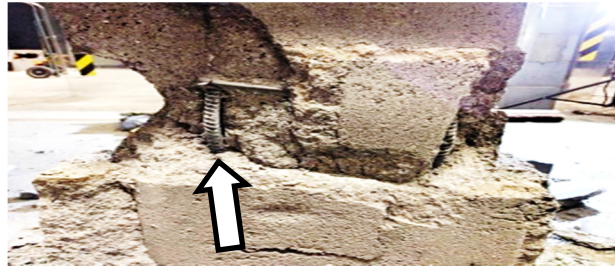


Figure 4: Rebar Buckling

Table 1 summarizes the results of concentric prism testing. Peak ultimate load represents the results of laboratory testing, taken as the output from the MTS machine. Overall, the reinforced specimens had a consistently higher strength than the unreinforced, grouted specimens. The difference in the compressive strength of the un-reinforced grouted specimens and reinforced specimens was approximately 4.5%, which is reasonable since the percentage of longitudinal steel in the prism is relatively small, 0.8%. The most significant contribution of the cage is in the failure mode, in which the core of reinforced specimens had more structural integrity at failure (Fig. 2).

The nominal strength of the block was 15 MPa; however, the tabulated values indicate that the block strength was higher than 15 MPa, since the grouted masonry average strength (f'_m) was calculated as 21.0 MPa. In comparison, the ungrouted masonry strength was assessed as 12.6 MPa. The effective area of the hollow prisms, A_e , was assessed using only the effective face shell thickness since the prisms were constructed with alternating open ends.

Table 1: Concentric Test Results (15 MPa Units)

SPECIMEN	PEAK ULTIMATE LOAD (kN)		
	REINFORCED GROUTED ($A_g = 74,100 \text{ mm}^2$)	UNREINFORCED GROUTED ($A_g = 74,100 \text{ mm}^2$)	HOLLOW ($A_e = 27,300 \text{ mm}^2$)
1	1,968	1,663	313
2	1,696	1,543	338
3	1,517	1,785	383
4	1,334	1,162	380
5	---	1,642	---
Average Ultimate Load (kN)	1,629	1,559	344
Std. Deviation (kN)	234	213	29
Coefficient of Variation (%)	14.4	13.7	8.3

--- Prism with fabrication defects / failed before testing

As noted earlier, two of the specimens in the first series were not tested concentrically. One hollow specimen failed during transportation to the testing machine and one reinforced specimen exhibited a large void at the bottom due to inadequate grout penetration. The void in this prism was filled with fast-setting, high-strength, no-shrinkage mortar, and used to evaluate the performance of the setup prepared to conduct eccentric tests.

ECCENTRIC TESTS RESULTS

Data points obtained at two different eccentricities ($e=t/3$ and $e=5t/12$) are superimposed on theoretical P-M interaction diagrams calculated for the prism in Fig. 6. Four points obtained from concentric tests are also plotted. Two interaction diagrams are presented, one corresponding to $f'_{m,gr} = 21.0$ MPa and another for $f'_{m,hollow} = 12.6$ MPa. The experimental data shows an acceptable correlation between the experimental data and the predicted P-M response in terms of a general trend. For the materials and block type used in this study, using $f'_{m,gr}$ would lead to unconservative results – using $f'_{m,hollow}$ would allow for a safer prediction of strength, since $f'_{m,hollow}$ is smaller than $f'_{m,gr}$. This could be attributed to factors related to the strength of the block relative to the grout and mortar materials, and also to the fact that the units were open in one side (Fig. 1), perhaps altering the failure mode when compared to conventional closed-cell units. These factors warrant further investigation in future studies.

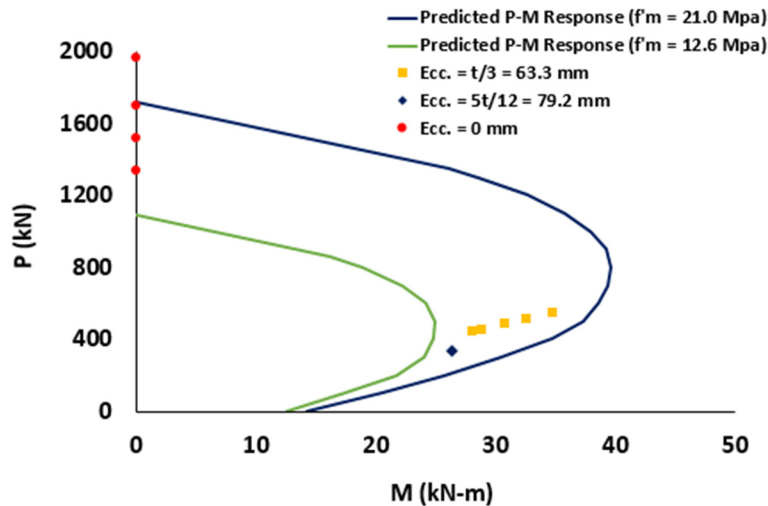


Fig. 6: Eccentric Test Results

The data points in Fig. 6 correspond to prisms with no visible fabrication defects. Results from prisms with apparent construction defects were not included since premature failures were observed, even though they were repaired. In other cases, prisms that had no visible voids revealed defects once the face shell spalled. Results from these prisms were also removed. Rebar buckling was not observed in any of the eccentrically tested prisms.

Qualitative observations made at each test eccentricity are described next, including prisms that had fabrication defects. Prisms tested at an eccentricity $t/6 = 31.7$ mm displayed a similar failure

mechanism (Fig. 7). Cracks developed initially in the face shell on the compression side prior to reaching the ultimate load. When successive load was applied, the face shells spalled. The cores of all the prisms tested at an centricity of $t/6$ remained mostly intact.



Figure 7: Failure modes ($e = t/6$)

At peak load, prisms tested at an eccentricity of $t/3$ exhibited a crack in the compression face shell. Upon development of a crack, a part of the face shell on the compression side of the prism became detached (Fig. 8).



Figure 8: Eccentric Prism Failure ($e = t/3$)

Prisms tested at an eccentricity of $5t/12$ exhibited little damage at ultimate load (Fig. 9). At peak load, the faceshell broke away from the core, initiating collapse.



Figure 9: Eccentric Prism Failure ($e = 5t/12$)

P-M Response Comparison

To investigate the performance of a prism with a reinforcing cage with respect to design scenarios using bars at the mid-section, the P-M interaction response of a 190mm x 390 mm section with a reinforcing cage made of 4-10M (400 mm^2) bars is compared with that of prisms reinforced at the

middle with one or two bars of different sizes, providing steel areas ranging between 100mm^2 to 600mm^2 . Figure 10 displays the superimposed P-M diagrams. Figures A, B, and C demonstrate that the innovative prism has a higher moment capacity than conventional prisms reinforced with a single 10M, 15M, or 20M bar over the entire range of axial load. Figures D, and E demonstrate that the innovative prism has a higher moment capacity than prisms reinforced with (2) - 15M or (2) - 20M bars for a range of axial load from 0.2 P_{max} to 0.75 P_{max} .

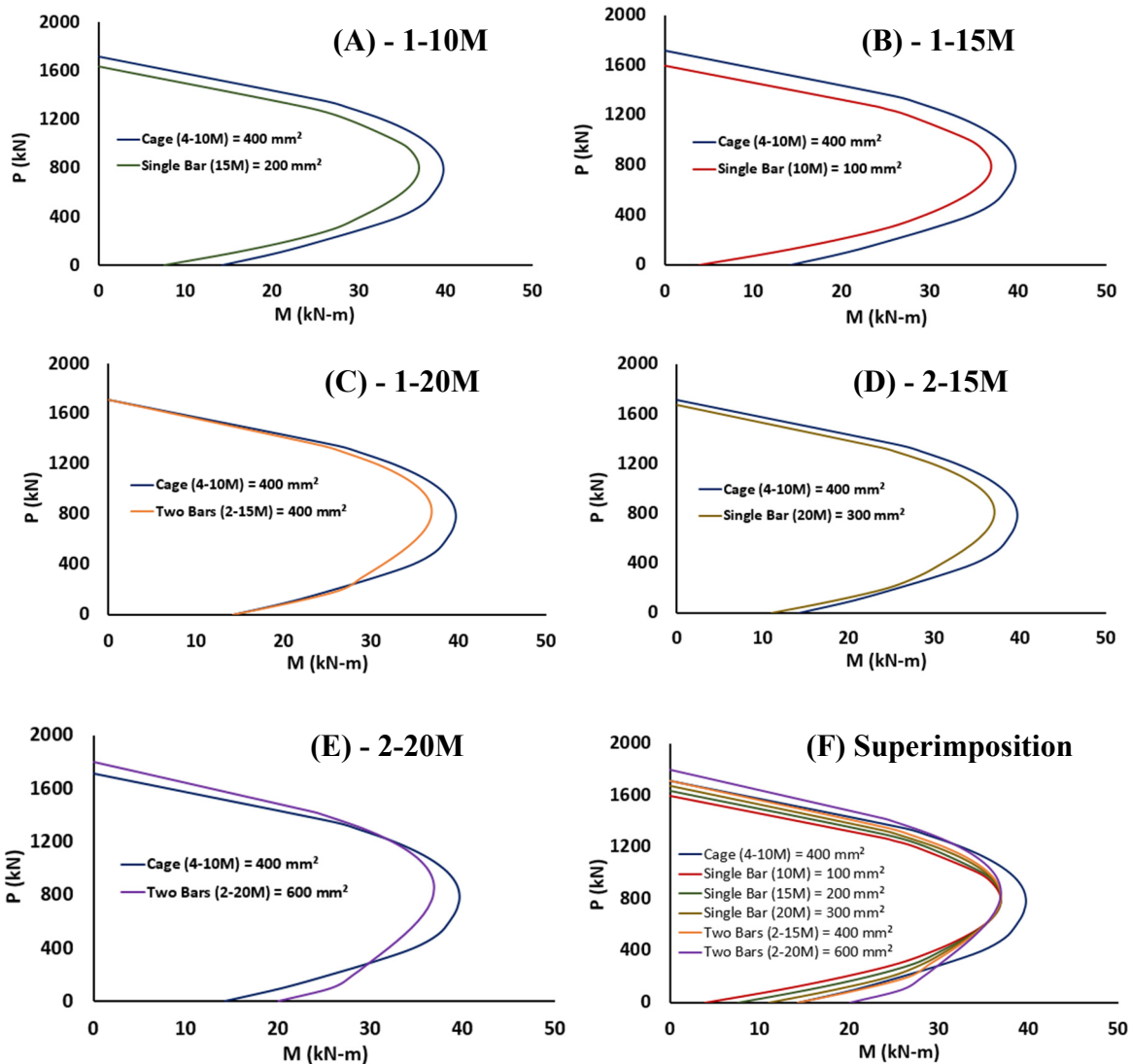


Figure 10: P-M Interaction Diagrams

PRELIMINARY FINITE ELEMENT MODEL (TALL WALL)

Fig. 11 depicts a schematic of a masonry wall reinforced with an in-line boundary element to be tested in a future phase of this study. The slenderness ratios targeted in that study will exceed 30; conditions for which the S304 code requires special design details to ensure ductile behaviour and to prevent buckling failures. As an aid in the design of full scale wall and wallet specimens, a

preliminary finite-element analysis model for OOP walls was developed and validated with experimental results. The experimental data selected for comparison was the lateral pressure vs. mid-span deflection of three 7.32 m x 1.20 m tall walls tested under gravity load (4.67 kN/m) and lateral pressure from an air bag [11]. The walls were made with 15cm blocks, fully grouted, and 5-#4 (12.7 mm diam.) reinforcing bars placed at the middle of the cells were the longitudinal reinforcement. The masonry compressive strength was 21.3 MPa.

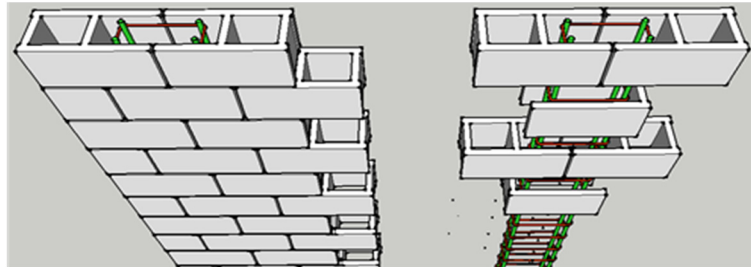


Figure 11: Tall Wall Reinforced with In-Line Boundary Element

Finite-Element Model

The tall wall modelling described in this section was conducted using the Open System for Earthquake Engineering Simulation (OpenSees) program [12]. OpenSees is an object-oriented software framework for simulation applications in earthquake engineering using finite element methods which has been shown to be able to accurately predict the response of highly nonlinear systems [13]. The masonry behaviour was assumed to be similar to that of concrete. Nonlinear material “Concrete02” was used to represent masonry, which includes tensile capacity with tension softening effects. It is a Kent-Scott-Park concrete model [14] with degrading linear unloading/reloading stiffness as per the work of Karsan-Jirsa [15]. The model was built using a series of interconnected “nonlinearBeamColumn” elements with distributed plasticity along their length. Each element has a fibre-based section as shown in Fig. 12, in which the element is discretized into a number of fibres (100) in the out-of-plan direction. The boundary conditions were set up as pinned-pinned. The model outline and the measured vs. calculated response is shown in Fig. 13.



Figure 12: Section Discretization

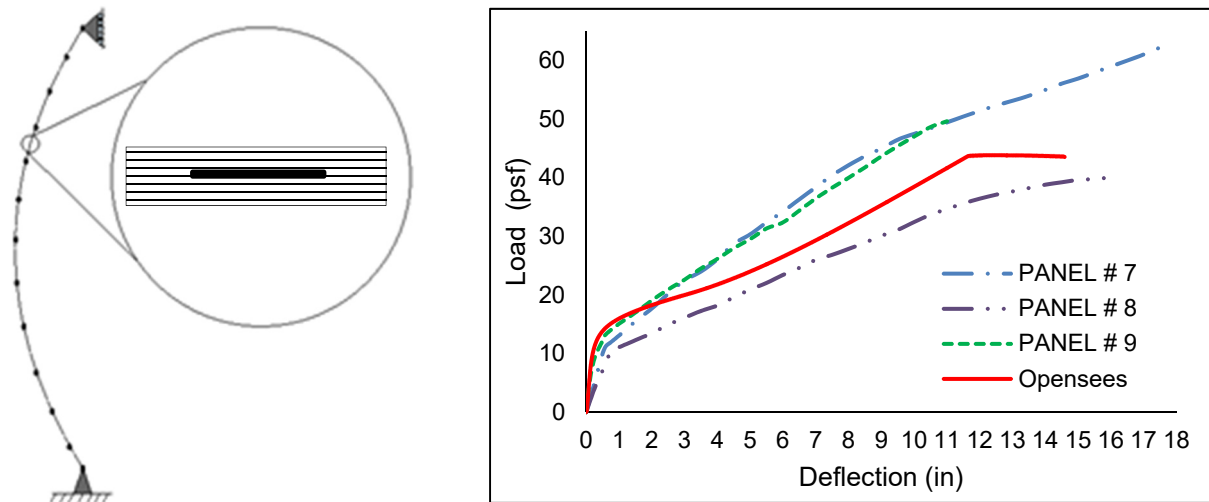


Figure 13: Finite element model of wall and performance

The results indicate that the model has a satisfactory correlation between measured and calculated results, predicting with reasonable accuracy the experimental response of tall walls. This shows that the model can be used to study and assist in the design of slender OOP masonry walls with different reinforcement arrangements.

CONCLUSIONS

This paper presents the results obtained from two series of masonry prisms tested under concentric and eccentric axial load. A total of 13 prisms were tested concentrically and 12 prisms were tested eccentrically. Prism fabrication showed that the innovative in-line boundary element can be fabricated with minimal deviation from common masonry practice. Under concentric axial load, reinforced prisms had a better structural performance, in terms of core integrity, than specimens with no reinforcing cage, which is a promising feature for the use of the innovative prism in tall walls. P-M interaction plane-section compatibility analyses show that prisms with reinforcing cages have enhanced moment capacities for comparable levels of axial load for a wide range of design variables. This was verified through eccentric testing. Further research is required to investigate the relationship between tie spacing, confinement of grouted core, and buckling. Preliminary analysis models show that finite-element tools can be effectively used to simulate slender masonry walls and assist in the design of future phases of this study.

ACKNOWLEDGEMENTS

Financial support for this research was provided by the NSERC Engage Grant program. Technical assistance was provided by M. Guzman from the Canadian Masonry Design Centre (CMDc) and Dr. M. Hagel from the Alberta Masonry Council (AMC). The Masonry Contractors Association of Alberta (MCAA) contributed labour, resources, and technical expertise. Mr. C. Pettit collaborated in the design of the experiment. The authors would like to thank these contributors for their support.

REFERENCES

- [1] Canadian Standards Association (2004). "Design of Masonry Structures." *CSA S304.1-04*. Rexdale, ON, Canada
- [2] Hamid. Ahmad A., Abboud. Bechara E., Farah. Muris W., Hatem. Michel K., Harris, Harry G., "Response of Reinforced Block Masonry Walls to Out-of-Plane Static Loads," Drexel University, September 1989, Philadelphia.
- [3] Tumialan, J. G. and Nanni, A. (2002). "Strengthening of Masonry Walls with FRP Bars." *Composites Fabricator Magazine*.
- [4] Korany, Yasser. and Drysdale, Robert. (2006). "Rehabilitation of Masonry Walls Using Unobtrusive FRP Techniques for Enhanced Out-of-Plane Seismic Resistance." *Journal of Composites for Construction.*, 10(3), 213-222.
- [5] Mierzejewski, Wojciech. (2010). *Out-of-Plane Bending of Masonry Walls with Near Surface-Mounted and Externally-Bonded Corrosion-Resistant Reinforcement*, Queen's University, Kingston, ON, Canada
- [6] Banting, B. R. and El-Dakhkhni, W. W. (2014). "Seismic Performance Quantification of Reinforced Masonry Structural Walls with Boundary Elements." *J. Struct. Eng.*, 140(5), 1477-1491.
- [7] Cyrier, Willis Bradford. (2012). *Performance of Concrete Masonry Shear Walls with Integral Confined Concrete Boundary Elements*, Washington State University, Pullman, WA, USA
- [8] Banting, Bennett Ralph. (2013). *Seismic Performance Quantification of Concrete Block Masonry Structural Walls with Confined Boundary Elements and Development of the Normal Strain-Adjusted Shear Strength Expression (NSSSE)*, McMaster University, Hamilton, ON, Canada
- [9] Drysdale, Robert G. and Hamid, Ahmad A. (1983). "Capacity of Concrete Block Masonry Prisms Under Eccentric Compressive Loading." *ACI Journal.*, 102-108
- [10] Ross, David Michael. (2013). *Recalibration of the Unit Strength Method for Determining the Compressive Strength of Grouted Concrete Masonry*, University of Alberta, Edmonton, AB, Canada
- [11] ACI-SEASC Task Committee on Slender Walls, "Test Report on Slender Walls," American Concrete Institute and the Structural Engineers Association of Southern California, February 1980-September 1982, Los Angeles.
- [12] McKenna, F. Fenves, G. Scott, H. Jeremic, B. (2000). "Open system for earthquake engineering simulation (OpenSees) [computer software]. Pacific Earthquake Engineering Research Center, University of California at Berkeley, California, USA.
- [13] Nelson, R., Saiidi, M., and Zadeh, S. (2007), "Experimental evaluation of performance of conventional bridge systems", Technical Rep. No. CCEER-07-4, Center for Civil Engineering Earthquake Research, Dept. of Civil Engineering, Univ. of Nevada, Reno, Nev.
- [14] Kent, D. C., and Park, R. (1971), "Flexural members with confined concrete", *J. Struct. Div.*, ASCE, 97(7), pp. 1969-1990.
- [15] Karsan, I. D., and Jirsa, J. O. (1969), "Behavior of concrete under compressive loadings", *J. Struct. Div.*, ASCE, 95(ST12), 2543-2563.